Communication

Not peer-reviewed version

Effect of Substrate Temperature on Weld Track Geometry in Directed Energy Deposition: A Comprehensive Investigation and Regression Modeling of processing 316L

Stefan Gnaase * , Artur Walter , Robin Rohling , Thoas Tröster

Posted Date: 25 April 2024

doi: 10.20944/preprints202404.1587.v1

Keywords: additive manufacturing; direct energy deposition; laser metal deposition; DED; LMD; 316L; 1.4404

Article

Effect of Substrate Temperature on Weld Track Geometry in Directed Energy Deposition: A Comprehensive Investigation and Regression Modeling of processing 316L

Stefan Gnaase *, Artur Walter, Robin Rohling and Thomas Tröster

Institute for Lightweight Design with Hybrid Systems (ILH), Automotive Lightweight Design (LiA), Paderborn University, Warburger Str. 100, 33098 Paderborn, Germany
* Correspondence: stefan.gnaase@upb.de

Abstract: This paper investigates the effects of various process parameters, specifically the substrate temperature, on weld track geometry in Directed Energy Deposition (DED) processes. A specialized experimental setup integrated within a DED machine facilitates controlled thermal conditioning of sample sheets. Through Design of Experiments (DoE) methods, individual weld marks are generated and analysed to assess geometric characteristics. Regression models are constructed to predict machine parameters for desired weld geometry at different substrate temperatures. Validation experiments confirm the accuracy and reliability of the regression models. Results show a consistent trend towards target geometric features across a broad range of substrate temperatures. Despite deviations in measured values, successful fabrication is achieved, demonstrating robust bonding between weld and substrate. Contact angle predictions exhibit precision within a partial temperature range for proper deposition. The developed model offers insights for optimizing DED process parameters to achieve desired weld characteristics, advancing the capabilities and reliability of additive manufacturing technology. Future work aims to refine the regression model and explore additional mathematical relationships for enhanced accuracy. An implication of this work is the potential to vary the local mechanical properties of parts by controlling the temperature profile while maintaining consistent geometric characteristics. By manipulating the substrate temperature, it may be possible to tailor the microstructure and mechanical properties of fabricated components in the future to meet specific requirements in different regions of the part.

Keywords: additive manufacturing; direct energy deposition; laser metal deposition; DED; LMD; 316L; 1.4404

1. Introduction

In the realm of additive manufacturing, particularly in the DED process, achieving precise control over weld seam geometry is one crucial factor for ensuring structural integrity and functional performance of fabricated components [1]. To this end, understanding the intricate interplay between process parameters and resulting weld characteristics is indispensable. In this paper, we present comprehensive investigations focused on elucidating the effects of various machine parameters and specifically the temperature of the substrate on weld track geometry in DED processes. The experimental setup employed in this study integrates a specialized apparatus for heating of sample sheets within the workspace of the DMG MORI LT65 3D DED machine. This setup facilitates controlled thermal conditioning of the samples, essential for reproducible experimentation.

In previous studies [2–4], researchers investigated the impact of temperature on DED processes. However, they did not address the broader scope covered in this work. Here, we focus on developing a comprehensive model to ensure consistent weld geometry across a wide substrate temperature

 doi:10.20944/preprints202404.1587.v1

range, up to 800 °C. Key process parameters including laser power, traversing speed, powder mass flow, and substrate temperature are therefore methodically altered to examine their influence on weld track geometry. Utilizing Design of Experiments (DoE) methods, a total of 360 individual weld marks are generated and analyzed. The geometric characteristics of each weld track, including height, width, dilution and contact angle, are assessed through incident light microscopy. Subsequently, the acquired data is employed to construct regression models, enabling the prediction of suiting machine parameters for a desired weld geometry at different substrate temperatures. Validation of the regression models is conducted through additional experiments, where machine parameters are determined based on target geometry specifications. Results of these validation experiments, along with their comparison to the specified values, provide insights into the accuracy and reliability of the regression models. Through this systematic investigation, we aim to enhance the understanding of the intricate relationships between process parameters and weld track geometry in DED processes. The findings presented herein offer valuable insights for optimizing DED process parameters to achieve desired weld characteristics, thereby advancing the capabilities and reliability of this additive manufacturing technology.

2. Materials and Methods

The following section of this work gives a brief introduction into the here used additive manufacturing technology DED. Finally, the experimental setup and procedures are explained.

2.1. Directed Energy Deposition (DED)

The DED process is characterized by the simultaneous delivery of powder and laser onto a substrate. As shown in **Figure 1**, metal powder in the form of particles is carried within an inert gas flow through the channels of a coaxial nozzle. A laser heat source, directed through the inner opening of the nozzle, creates a locally allocated melt pool on a chosen substrate. The fine metal powder particles are then melted within the melt pool and fused to the substrate. By placing welds next to each other and stacking the created layers, a 3D object is created. Besides creating whole 3D parts, the process can also be used to repair high-value parts by, e.g., filling in worn-out regions of a die-cast tool. By facilitating special powder delivery systems, it is also possible to change or mix different powders during the process to create graded materials. The particle size of typically used powder in the DED process ranges between 50 and 150 µm [5]. It should be noted that there is a variety of different names for the DED-Process in the literature [6]. [7] gives a good overview about the used terms in the literature for the interested reader.

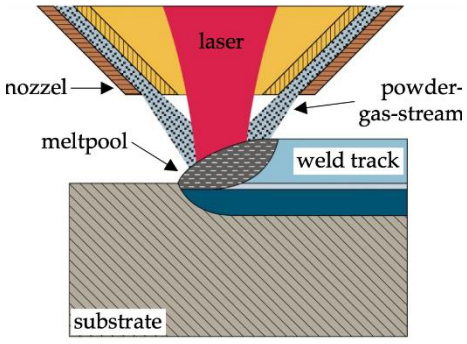

Figure 1. Schematics of the DED process [5].

2.2. Experimental Setup

To conduct the experiments, a dedicated apparatus for precise heating of the samples was integrated within the workspace of the DMG MORI LT65 3D DED machine (see **Figure 2a**). This apparatus comprises a ceramic body designed to securely accommodate the sample sheets, thereby providing both thermal insulation and electrical isolation from the ambient environment. The sample sheets are affixed onto the ceramic body through the utilization of water-cooled electrodes, which are

 doi:10.20944/preprints202404.1587.v1

secured by toggle levers. Each sample sheet measures 30 x 170 x 3 mm and is composed of the material 1.4404. For resistive heating, a welding transformer delivering a peak current of 630 A at a voltage of 4.85 V was used. The temperature of the sample sheets was monitored utilizing an infrared camera (Optris Pl400i) in conjunction with a thermocouple. The used nozzle was the machines standard COAX14 AA13 nozzle.

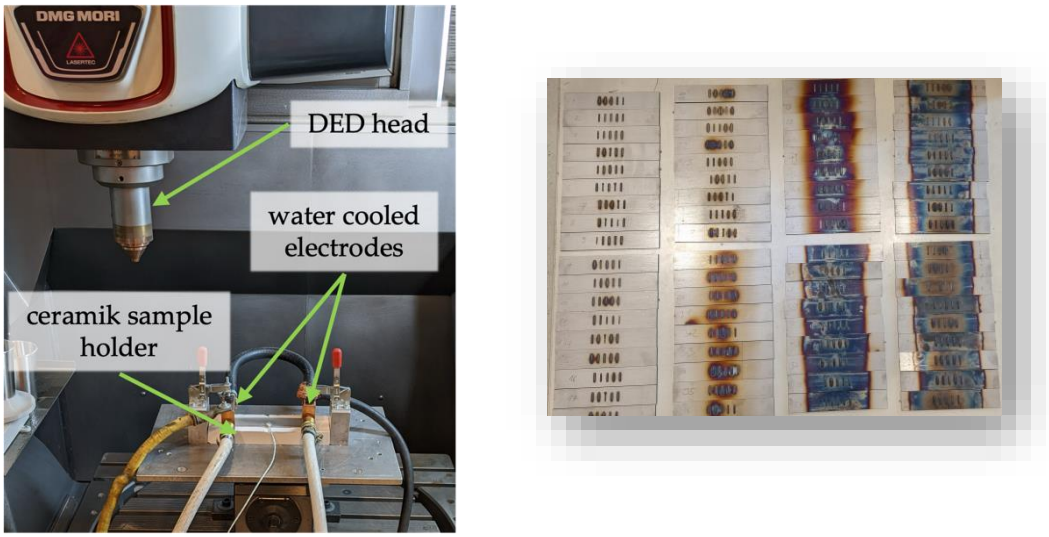

(**a**) (**b**)

Figure 2. Experimental setup and samples: (**a**) experimental setup; (**b**) Samples sorted in ascending bins by substrate temperature in zig-zag-fashion (Start: Upper Left Corner → down → right & up).

2.3. Experimental Procedure

The experimental protocol commenced with the initiation of the welding program for the application of individual weld tracks, with the laser head positioned just prior to the starting point of the operation. Subsequently, the feed rate was manually adjusted to 0%, and the sample sheet was heated to approximately 50°C above the target temperature. Once the temperature of the sample sheet approached within a range of ±5°C of the target temperature, as determined through temperature measurements, the feed rate was reinstated to 100%, and the program execution was thereby initiated. Following the heating phase, five individual welding tracks, each measuring 20 mm in length, were deposited onto the preheated substrate under identical powder mass flow rate conditions. The parameters for the welding tracks were systematically varied as outlined below:

1. laser power in W: 500, 1000, 1500, 2000, 2500
2. traversing speed in mm/min: 400, 800, 1200
3. powder mass flow in g/min: 5, 12.5, 20
4. substrate temperature in °C: RT, 100, 200, 300, 400, 600, 800, 1000

The experimental setup as well as the experimental outcome is shown in **Figure 1**.

Using DoE-Methods, the parameters were combined and experiments with the chosen combinations were conducted. The resulting 360 individual weld marks were first separated orthogonal to the direction of application and embedded, ground, polished and etched using V2A etching component (hydrochloric acid fuming 37%: 500 ml/l, nitric acid >65%: 50 ml/l, Dr. Vogel's economy etch: 1.5 ml/l) for further investigations. Stitched images of the weld track cross-section were then taken using an incident light microscope (Keyence digital microscope VHX5000) with 200 times magnification. This images then were used to determine the geometric characteristics analog to the literature [2,8–11] as shown in **Figure 2**.

The data obtained was then used to create a regression model to make specific predictions about the machine parameters required for different desired geometric characteristics. The ones chosen

 doi:10.20944/preprints202404.1587.v1

were bead width and height, dilution and contact angle of individual weld seams at different substrate temperatures. The contact angle has been measured at both sides of the weld and used to form a mean value. To approximate the level of dilution the ratio between the area of the molten substrate Material (4.) and the total area of molten material (3. + 4.) is used.

$$Dilution = \frac{4.}{3. + 4.} \quad (1)$$

The "Minitab 2018" software was then used to create regression functions. The boundary conditions are defined as follows:

Responses

- Travel speed
- Laser power
- Contact angle

Continuous predictors

- Bead width
- Bead height
- Dilution
- Substrate temperature
- Powder mass flow

All other settings within the software have been left as standard. The contact angle response is used as a check to ensure that the contact angle is within a specified tolerance range of > 90 °. As mentioned in the work of [12], contact angles of near 90° or below are not desirable since they can lead to a higher probability for lack of fusion defects with the substrate. Another, more recent work suggests that for a fully dense component outcome, the contact angle should be between 120 and 140 ° [13]. As the powder mass flow rate is not a directly controllable process variable, it was assumed here as a predictor as it can be kept constant during the process. The model can therefore be used to specify the desired target geometry in the form of seam width, height, and dilution. With knowledge over the desired powder mass flow and the substrate temperature, the traversing speed and laser power required to generate these target variables will then be calculated using the developed regression functions.

3. Results

The measurement results of the conducted experiments were analyzed using correlation analysis. The Pearson correlation coefficients and the corresponding p-values resulting from the data are shown in **Table 1**.

Table 1. Correlationmatrix.

	Laser power	Feedrate	Powder mass flow	Substrate temp.	Bead width	Contact angle	Bead height
Feedrate	0.00						
	1.00						
					Cell contents:		
Powder mass flow	0.00	0.00			- *Correlation according to Pearson*		
	1.00	1.00			- *p-value*		
Substrate temperature	0.00	0.00	0.00				
	1.00	1.00	1.00				
Bead width	0.53	-0.23	0.11	0.26			
	0.00	0.00	0.04	0.00			
Contact angle	-0.26	-0.15	0.57	-0.34	-0.28		
	0.00	0.00	0.00	0.00	0.00		

 doi:10.20944/preprints202404.1587.v1

Bead height	0.10	-0.60	0.68	-0.01	0.49	0.61	
	0.06	0.00	0.00	0.91	0.00	0.00	
Dilution	0.64	0.03	-0.47	0.23	0.33	-0.61	-0.33
	0.00	0.64	0.00	0.00	0.00	0.00	0.00

The following main dependencies can be derived from this:

- Track width & laser power (0.527)
- Contact angle & powder mass flow (0.566)
- Track height & powder mass flow + feed rate (0.677 + -0.597)
- Dilution & laser power (0.638)

Thus, the track width increases with increasing laser power. The contact angle increases with increasing powder mass flow. The track height increases with increasing powder mass flow and decreases with increasing feed rate. The dilution increases with increasing laser power. Since the powder mass flow is not reliably controllable during the process – it must be calibrated before each print job – this process parameter will be kept constant. This leaves the feedrate and laser power as controllable process-parameters. The evaluation of the 360 experiments yielded the following regression functions for the responses travel speed, laser power, and contact angle:

$$\textbf{Feedrate} = 876{,}7 - 0{,}0327\ \text{bead width} - 0{,}6827\ \text{bead height} + 1{,}829\ \text{dilution} + 0{,}0002\ \text{substrate temperature} + 43{,}45\ \text{powder mass flow} \quad (1)$$

$$\textbf{Laser power} = -310 + 0{,}3367\ \text{bead width} - 0{,}0614\ \text{bead height} + 16{,}82\ \text{dilution} - 0{,}7274\ \text{substrate temperature} + 40{,}78\ \text{powder mass flow} \quad (2)$$

$$\textbf{Contact angle} = 94{,}63 - 0{,}01991\ \text{bead width} + 0{,}04392\ \text{bead height} - 0{,}1893\ \text{dilution} - 0{,}03146\ \text{substrate temperature} + 2{,}439\ \text{powder mass flow} \quad (3)$$

To validate the model, experiments were carried out in which the regression functions were used to determine the machine parameters for selected geometry target variables. In this experiment, we deposited five beads at each substrate temperature level, using identical process parameters. This mirrors the setup of the previous 360 experiments, with a minor adjustment: we controlled the temperature between each bead and, if needed, waited for the substrate to cool before proceeding. The values for the continuous predictors and geometry target variables were chosen as 3 mm for the bead width, 1 mm for the bead height, 15% for the dilution, and 15 g/min for the powder mass flow at substrate temperatures of RT, 200, 400, 600, and 800°C. Choosing 15 g/min is the attempt of maximizing the material output while not fully utilizing the material transport capabilities of the machine. The height and width that has been chosen fits the literature requirement of an aspect ratio of 3 to 5 (aspect ratio = width / height) [14]. The resulting machine parameters can be found in **Table 2**:

Table 2. Answers to regressions functions at different substrate temperatures.

Substrate temperature °C	Feedrate mm/min	Laserpower W	Contact Angle °
RT	775.09	1485.865	111.77825
200	775.125	1358.57	106.2675
400	775.165	1213.09	99.9695
600	775.205	1067.61	93.6715
800	775.245	922.13	87.3735

As can be seen, the difference in feed rate is negligible compared to the laser power. However, according to the model, there is a significant difference in the resulting contact angle of the individual

 doi:10.20944/preprints202404.1587.v1

tracks, which must be considered in further investigations if it actually occurs. Three weld beads were produced for each parameter pair for model validation using the same experimental setup as before. The results of the investigations are shown in **Figure 3**.

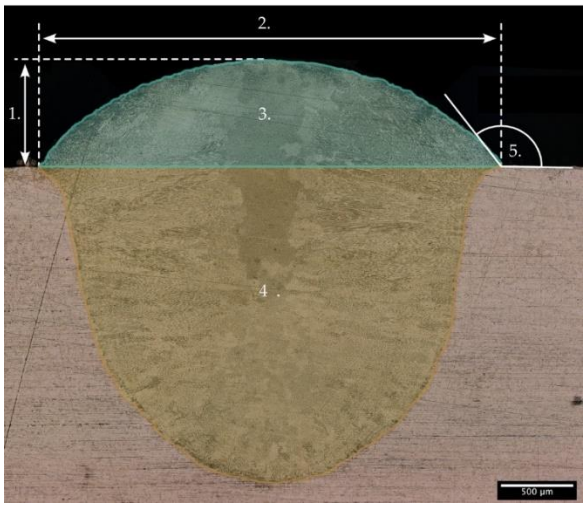

Figure 3. Cross-sectional image of a weld track with the measured geometric characteristics. 1: height, 2: width, 3: welded-on area above substrate surface, 4: welded-in area within substrate, 5: contact area.

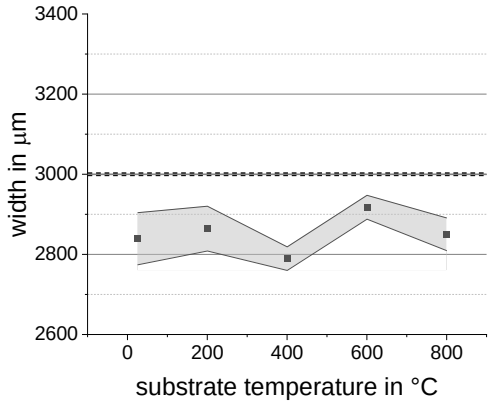

(**a**)

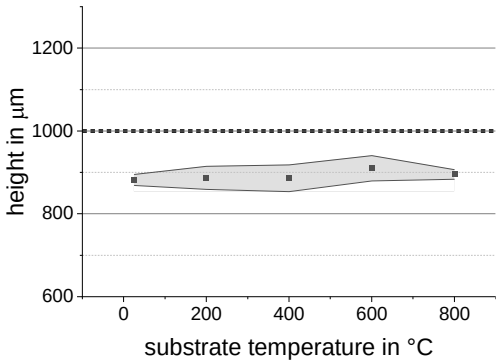

(**b**)

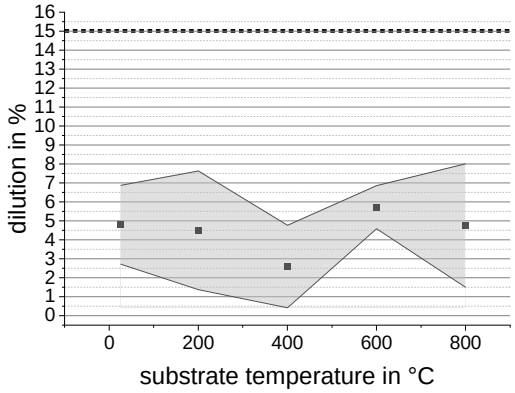

(**c**)

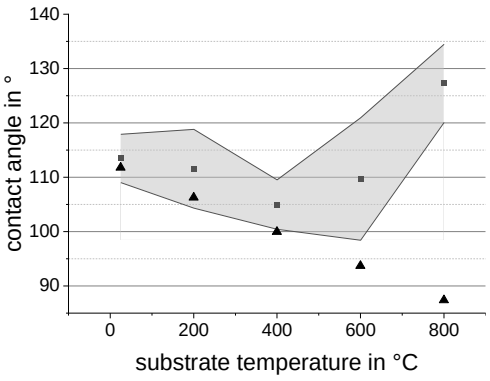

(**d**)

 doi:10.20944/preprints202404.1587.v1

Figure 4. Results of model validation experiments shown as error bands (squares indicate mean value, error-band derived from standard deviation) for individual welding bead bins with the desired quantities as horizontal dashed line and the anticipated contact angle values as triangles: (**a**) width; (**b**) height; (**c**) dilution; (**d**) contact angle.

4. Discussion

The results of the model validation indicate a deviation between the measured target variables and the specified values. However, it's important to note that the DED process typically exhibits a certain level of variability in results, particularly concerning weld bead heights and widths. This inherent variability is well-known in the field, and as such, the observed results can be considered sufficiently accurate. Notably, there is a consistent trend towards the target values of geometric features across the range of substrate temperatures, which aligns with the primary objective of this study. The maximum deviation of the mean measured value across the temperature range from the target value is 7% for width, 11.82% for height, and notably, 82.69% for dilution. While the significant deviation in dilution may initially raise concerns, it's essential to consider the practical implications. Despite the low measured dilution values, examination of cross-sectional images (**Figure 5**) reveals a robust bond between the weld and the substrate, demonstrating successful fabrication even with minimal measured dilution.

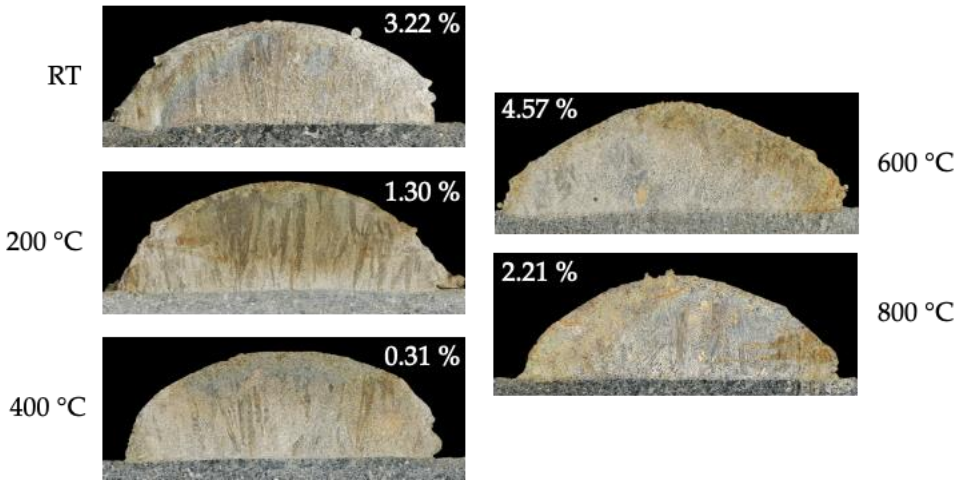

Figure 5. Images of cross-sectional cut weld beads, dilution in % in the upper part of pictures, substrate temperature adjacent to each picture.

Regarding the prediction of contact angles, the model demonstrates decent precision, particularly at room temperature and 200°C substrate temperatures, where the error band closely encompasses the predicted values. Although the model predicts a decrease in contact angle with increasing temperature, real-world investigations reveal a different trend. Nonetheless, the contact angles for each temperature level falls within the range necessary for proper deposition, spanning from 90 to 140 degrees.

In summary, the developed model effectively forecasts process parameters for different substrate temperatures, resulting in a consistent geometric outcome of individual weld beads. While adjustments may be necessary to enhance the accuracy of the prediction, the manufactured weld beads meet all criteria for the theoretical production of fully dense volumetric parts. Future endeavours should focus on refining the regression model using data from validation experiments and conducting a precise analysis of the relationships between process parameters and target values.

Author Contributions: For research articles with several authors, a short paragraph specifying their individual contributions must be provided. The following statements should be used "Conceptualization, S.G. and T.T.; methodology, S.G.; validation, A.W. and R.R.; investigation, S.G. A.W. and R.R.; writing—original draft

 doi:10.20944/preprints202404.1587.v1

preparation, S.G.; writing—review and editing, S.G.; supervision, T.T. All authors have read and agreed to the published version of the manuscript.

Conflicts of Interest: The authors declare no conflicts of interest.

References

1. Mani, M.; Lane, B.M.; Donmez, M.A.; Feng, S.C.; Moylan, S.P. A review on measurement science needs for real-time control of additive manufacturing metal powder bed fusion processes. *International Journal of Production Research* **2017**, *55*, 1400–1418, doi:10.1080/00207543.2016.1223378.
2. Heilemann, M.; Jothi Prakash, V.; Beulting, L.; Emmelmann, C. Effect of heat accumulation on the single track formation during laser metal deposition and development of a framework for analyzing new process strategies. *Journal of Laser Applications* **2021**, *33*, 12003, doi:10.2351/7.0000307.
3. Isquierdo, D.V.; Siqueira, R.; Carvalho, S.M.; Lima, M. Effect of the initial substrate temperature on heat transfer and related phenomena in austenitic stainless steel parts fabricated by additive manufacturing using direct energy deposition. *Journal of Materials Research and Technology* **2022**, *18*, 5267–5279, doi:10.1016/j.jmrt.2022.04.143.
4. Moheimani, S.K.; Iuliano, L.; Saboori, A. The role of substrate preheating on the microstructure, roughness, and mechanical performance of AISI 316L produced by directed energy deposition additive manufacturing. *Int J Adv Manuf Technol* **2022**, *119*, 7159–7174, doi:10.1007/s00170-021-08564-4.
5. Jambor, T. *Funktionalisierung von bauteiloberflächen durch Mikro-Laserauftragsschweißen*, 2012.
6. Mazzucato, F.; Tusacciu, S.; Lai, M.; Biamino, S.; Lombardi, M.; Valente, A. Monitoring Approach to Evaluate the Performances of a New Deposition Nozzle Solution for DED Systems. *Technologies* **2017**, *5*, 29, doi:10.3390/technologies5020029.
7. Saboori, A.; Aversa, A.; Marchese, G.; Biamino, S.; Lombardi, M.; Fino, P. Microstructure and Mechanical Properties of AISI 316L Produced by Directed Energy Deposition-Based Additive Manufacturing: A Review. *Applied Sciences* **2020**, *10*, 3310, doi:10.3390/app10093310.
8. Aleksandr, K.; Ferdinando, S.; Joel, R.; Joel, C.; Jordan, M.; Thomas, J. Effect of direct energy deposition parameters on morphology, residual stresses, density, and microstructure of 1.2709 maraging steel. *Int J Adv Manuf Technol* **2021**, *117*, 1287–1301, doi:10.1007/s00170-021-07635-w.
9. Sreekanth, S.; Ghassemali, E.; Hurtig, K.; Joshi, S.; Andersson, J. Effect of Direct Energy Deposition Process Parameters on Single-Track Deposits of Alloy 718. *Metals* **2020**, *10*, 96, doi:10.3390/met10010096.
10. Sciammarella, F.; Salehi Najafabadi, B. Processing Parameter DOE for 316L Using Directed Energy Deposition. *JMMP* **2018**, *2*, 61, doi:10.3390/jmmp2030061.
11. Zhong, C.; Biermann, T.; Gasser, A.; Poprawe, R. Experimental study of effects of main process parameters on porosity, track geometry, deposition rate, and powder efficiency for high deposition rate laser metal deposition. *Journal of Laser Applications* **2015**, *27*, doi:10.2351/1.4923335.
12. Borovkov, H.; La Yedra, A.G. de; Zurutuza, X.; Angulo, X.; Alvarez, P.; Pereira, J.C.; Cortes, F. In-Line Height Measurement Technique for Directed Energy Deposition Processes. *JMMP* **2021**, *5*, 85, doi:10.3390/jmmp5030085.
13. Javidrad, H.; Aydin, H.; Karakaş, B.; Alptekin, S.; Kahraman, A.S.; Koc, B. Process parameter optimization for laser powder directed energy deposition of Inconel 738LC. *Optics & Laser Technology* **2024**, *176*, 110940, doi:10.1016/j.optlastec.2024.110940.
14. Michael Cornelius Hermann Karg; Oliver Hentschel; Bhrigu Ahuja; Daniel Junker; Ulf Hassler; Claus Schäperkötter; Andreas Haimerl; Horst Arnet; Marion Merklein; Michael Schmidt. *Comparison of process characteristics and resulting microstructures of maraging steel 1.2709 in Additive Manufacturing* via *Laser Metal Deposition and Laser Beam Melting in Powder Bed*, 2016.